JOURNAL OF SMOOTH MUSCLE RESEARCH

J. Smooth Muscle Res. 2021; 57: 8–18
Published online: April 20, 2021; doi: 10.1540/jsmr.57.8

Original

Glycogen accumulation in smooth muscle of a Pompe disease mouse model

Angela L. McCALL[1], Justin S. DHINDSA[1], Aidan M. BAILEY[1], Logan A. PUCCI[1], Laura M. STRICKLAND[1] and Mai K. ElMALLAH[1]

[1]*Division of Pulmonary Medicine, Department of Pediatrics, School of Medicine, Duke University, Durham, NC 27710, USA*

Submitted January 14, 2021; accepted in final form March 4, 2021

Abstract

Pompe disease is a lysosomal storage disease caused by mutations within the *GAA* gene, which encodes acid α-glucosidase (GAA)—an enzyme necessary for lysosomal glycogen degradation. A lack of GAA results in an accumulation of glycogen in cardiac and skeletal muscle, as well as in motor neurons. The only FDA approved treatment for Pompe disease—an enzyme replacement therapy (ERT)—increases survival of patients, but has unmasked previously unrecognized clinical manifestations of Pompe disease. These clinical signs and symptoms include tracheo-bronchomalacia, vascular aneurysms, and gastro-intestinal discomfort. Together, these previously unrecognized pathologies indicate that GAA-deficiency impacts smooth muscle in addition to skeletal and cardiac muscle. Thus, we sought to characterize smooth muscle pathology in the airway, vascular, gastrointestinal, and genitourinary in the *Gaa*$^{-/-}$ mouse model. Increased levels of glycogen were present in smooth muscle cells of the aorta, trachea, esophagus, stomach, and bladder of *Gaa*$^{-/-}$ mice, compared to *wild type* mice. In addition, there was an increased abundance of both lysosome membrane protein (LAMP1) and autophagosome membrane protein (LC3) indicating vacuolar accumulation in several tissues. Taken together, we show that GAA deficiency results in subsequent pathology in smooth muscle cells, which may lead to life-threatening complications if not properly treated.

Key words: Pompe disease, smooth muscle, autophagy

Background

Pompe disease is a glycogen storage disease (GSD) caused by mutations within the gene encoding acid α-glucosidase (GAA)—an enzyme responsible for hydrolyzing lysosomal glycogen (1). Patients with Pompe disease develop systemic accumulation of lysosomal glycogen in cardiac and skeletal muscle as well as in mo-

Corresponding author: Mai K. ElMallah, Division of Pulmonary Medicine, Department of Pediatrics, Duke University Medical Center, Box 2644, Durham, NC 27710, USA
E-mail: mai.elmallah@duke.edu
(Supplementary material: refer to PMC https://www.ncbi.nlm.nih.gov/pmc/journals/3118/)

tor neurons (2–4). Symptom severity depends on the degree of residual GAA activity; severe (infantile-onset, IOPD) cases have less than 1% of GAA activity and less severe (late-onset, LOPD) cases have >1% residual GAA activity (3, 5, 6). The only FDA approved treatment for Pompe disease is an enzyme replacement therapy (ERT) of recombinant human GAA (rhGAA), which prolongs survival. However, as patients survive longer, latent smooth muscle pathology, leading to significant morbidity and mortality is unmasked (7–10).

Persistent smooth muscle pathology has a substantial impact on quality of life (QoL) and leads to life-threatening complications. Case reports describe LOPD patients who underwent emergency bronchoscopies and found up to 90% occlusion of the distal trachea and bronchi, which then required a stent to hold the airway open (7, 11). In addition to airway smooth muscle weakness, vascular deterioration, gastrointestinal (GI) discomfort, and loss of genitourinary (GU) control has also been observed. Cerebral and aortic aneurysms have caused microhemorrhages leading to symptoms ranging from headaches and numbness, to coma and death (8, 12–18). Clearly, GI and GU symptoms negatively impact on patient QoL. Furthermore, symptoms of poor feeding, chronic gastroesophageal reflux, and urinary bladder infections can evolve into substantial health complications.

Our group recently described glycogen accumulation and dysfunction of airway smooth muscle in the *Gaa*$^{-/-}$ mouse (19). When exposed to methacholine, a bronchoconstrictive agent, these mice failed to respond, indicating impaired airway contractility. In addition, when bronchi of these mice were evaluated *ex vivo*, contractile force was significantly reduced compared to *wild type* (WT) littermates. In the present study, we further expand on smooth muscle pathology by investigating vascular, GI, and GU smooth muscle. The mouse model used is GAA-deficient in all cell types and experiences many of the symptoms observed in Pompe patients and survives into adulthood (up to 6–9 months) without therapeutic intervention. We find glycogen, lysosomes, and autophagosomes are all amassed in various smooth muscle containing tissues of the *Gaa*$^{-/-}$ mouse. These findings have serious implications for the function of these tissues and the cellular transport of ERT for their repair.

Methods

Mice

Wild type (WT) B6;129 mice and *Gaa*$^{-/-}$/B6;129 (*Gaa*$^{-/-}$) mice (20) were bred and housed in accordance with Duke University Institutional Animal Care and Use Committee (IACUC). They were maintained with food and water available *ad libitum* and euthanized at 6 and 15 months of age.

GAA activity assay

Enzyme assay was performed as previously described (21–24). Briefly, extracted tissues were harvested, rinsed in PBS, and flash frozen in liquid nitrogen. Whole organs were homogenized in molecular grade water with protease inhibitor cocktail (VWR), using a FastPrep24 (MP Biomedicals) followed by three freeze/thaws. Non-homogenized materials were pelleted, and clarified lysate was maintained at −80 °C. Five µl of each sample was incubated with 4-methylumbelliferyl-α-D-glucosidase (Millipore-Sigma) for 1 h at pH 4.3. Fluorescence resulting from substrate cleavage was detected with a Tecan Multimode Plate Reader and coordinating Magellan Software. Sample readings were compared to a standard curve generated from 4-methylumbelliferone (Millipore-Sigma). All samples were normalized to protein levels determined by DC Protein Assay (Bio-Rad), performed in accordance with the manufacturer's protocol.

Glycogen assay

Molecular glycogen assay was performed using the Abcam (ab65620) kit as directed. Briefly, 2–10 mg of tissue was homogenized in molecular grade water with protease inhibitor, using a FastPrep24. Homogenate was heated at 95 °C for 10 min, then clarified by centrifugation (13,000 rpm, 10 min, 4 °C). The supernatant was diluted between 1:50–1:100 in Hydrolysis Buffer. 4 µl of diluted sample was mixed with 1 µl of Hydrolysis Enzyme Mix in a clear 384 well plate, then incubated at room temperature for 30 min. 5 µl of Reaction Mix was added and the incubation was repeated. Absorbance at 570 nm was read on a NanoDrop™ One (ThermoFisher) with coordinating software. Samples were compared to a standard curve, and normalized to protein levels determined by DC Protein Assay (Bio-Rad), performed in accordance with the manufacturer's protocol.

Western blot

Whole organs were homogenized in RIPA buffer plus protease inhibitor (VWR) with a FastPrep (MPBiomedicals). They then underwent one freeze/thaw and were clarified by centrifugation twice to remove particulates. Proteins were separated on a 4–20% gel and transferred to PVDF membranes. Antibodies used: LAMP1 (DSHB 1D4B); LC3 (CST 4599); β-actin (CST 8457); GAPDH (CST 97166). Anti-rabbit (Invitrogen A21096) and anti-rat (Invitrogen A32735) AlexaFluor™ secondary antibodies were used for detection. Membranes were imaged with a Bio-Rad ChemiDocMP, then analyzed with coordinating Bio-Rad Image Lab Software. LAMP1, LC3-I, and LC3-II bands were quantified and normalized to GAPDH or β-actin.

PAS histology

Tissues were harvested and fixed in 2.5% glutaraldehyde in 0.1 M sodium cacodylate. They were then post-fixed in 1% osmium tetroxide, embedded in epoxy resin (EPON), and sectioned at 1 µm by the Duke Electron Research Electron Microscopy Core. Sections were stained with periodic acid-Schiff (PAS) (Sigma) according to manufacturer's protocol. All sections were imaged on a Leica DMRA Compound Light Microscope at 63× magnification.

Immunofluorescence

Tissues were harvested and embedded in OCT Compound and frozen in isopentane in liquid nitrogen. They were sectioned to 7 µm and stained as previously described (21). LAMP1 (DSHB 1D4B) and LC3 (Novus NB100-2200) antibodies were applied overnight and identified with anti-rat AlexaFluor™488 and anti-rabbit AlexaFluor™ 594 secondary antibodies (Invitrogen). Sections were imaged using an ECHO Revolve 4.

Statistics

In all molecular analyses (GAA Activity, Glycogen Quantification, and Western Blot), a Student's *t* test was used to evaluate significance. Significance was considered at a *P*-value of <0.05. Error bars represent mean ± S.E.M.

Ethics approval

The usage of mice in this study was approved by the Duke University Institutional Animal Care and Use Committee.

Results

GAA activity deficiency and glycogen accumulation

The mouse model used in this study is the most widely characterized mouse model of Pompe disease. It is a global knockout of *Gaa* through disruption of exon 6 (20). To confirm a lack of GAA protein, we performed an enzymatic activity assay on the aorta, trachea, esophagus, stomach, and bladder (Fig. 1A). In all tissues, WT mice had significantly higher levels of GAA activity, with negligible levels present in the $Gaa^{-/-}$ mice at 6 months of age. Mean WT levels of activity ranged from up to 110 nmol/ mg protein/h in the trachea to up to 55–60 nmol/ mg protein/h in the esophagus, stomach, and bladder to up to 40 nmol/ mg protein/h in the aorta.

In congruence with diminished GAA enzyme activity, the aorta, trachea, esophagus, stomach, and bladder of $Gaa^{-/-}$ mice all had significantly higher levels of molecular glycogen than WT controls at 6 months of age (Fig. 1B). $Gaa^{-/-}$ esophagus, trachea, and bladder had the highest levels of glycogen with mean values of 0.614 ± 0.127 μg/μg protein, 0.508 ± 0.062 μg/μg protein, and 0.324 ± 0.160 μg/μg protein, while the stomach had 0.151 ± 0.30 μg/μg protein and the aorta contained only 0.054 ± 0.017 μg/ug protein.

As Pompe disease progresses, lysosomes accumulate glycogen and disrupt the architecture of smooth muscle cells (25). To visualize the location of the glycogen in smooth muscle, epon-embedded tissue sections were stained with periodic acid-Schiff (PAS) reagents, which identify glycogen with bright pink/purple staining (Fig. 2). We observe large glycogen deposits throughout smooth muscle cells at 6 months in the esophagus and bladder (Fig. 2E and H; black arrows). A few small PAS+ puncta are also present at 6 months in the aorta (Fig. 2B). These glycogen deposits are in discrete puncta, congruent with lysosomal glycogen as observed in other tissues (22, 26, 27). The smooth muscle cells of WT controls are completely devoid of PAS+ puncta (Fig. 2A, D, G). We also evaluated glycogen accumulation in these tissues at 15 months of age (Fig. 2C, F, I). The

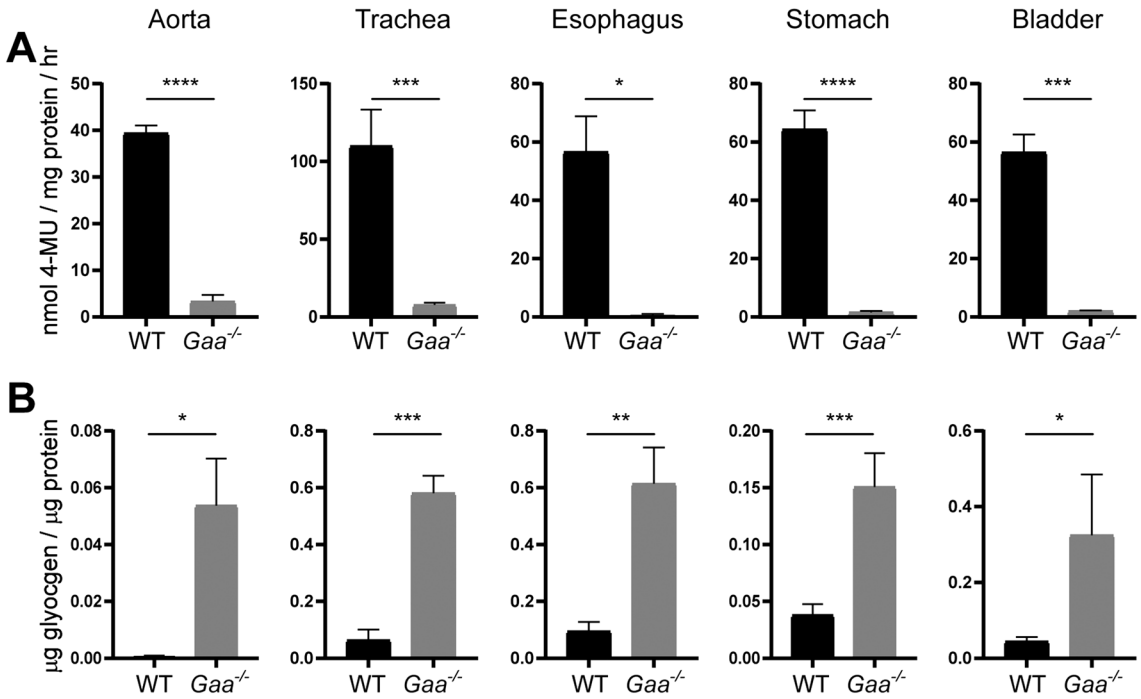

Fig. 1. Reduced GAA enzyme activity and increased glycogen in 6 month old $Gaa^{-/-}$ mice. (A) Significant levels of GAA enzyme activity are observed in the aorta, trachea, esophagus, stomach, and bladder of WT mice. (B) 6-month-old $Gaa^{-/-}$ mice have significant glycogen accumulation within smooth muscle-containing tissues. n=3–6 per group. Error bars represent mean ± SEM. **P*<0.05, ***P*<0.01, ****P*<0.001, *****P*<0.0001.

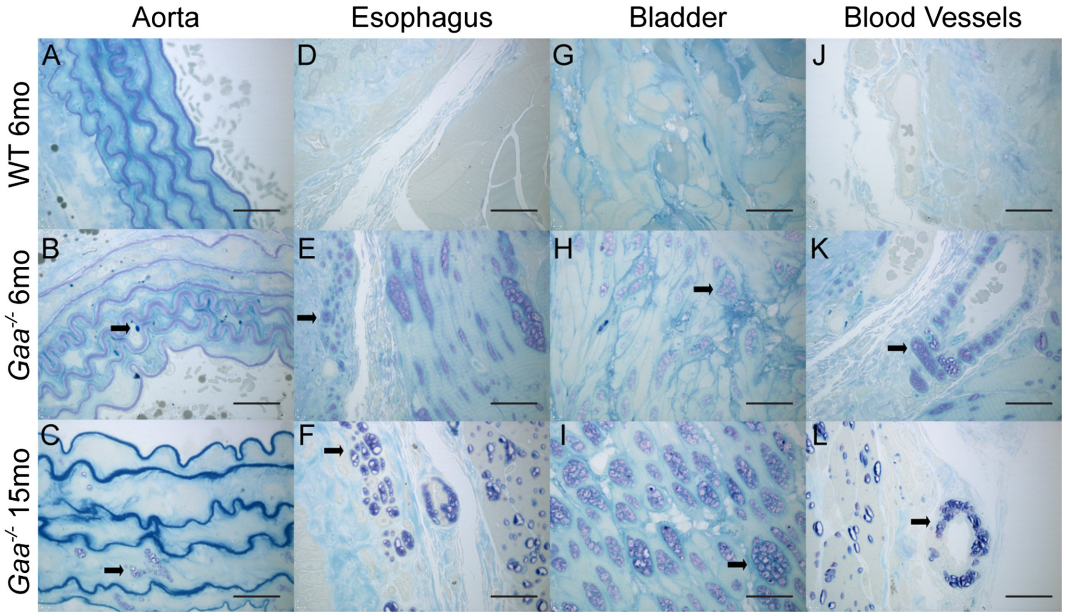

Fig. 2. Glycogen deposits found within smooth muscle of 6- and 15-month-old *Gaa*$^{-/-}$ mice. Representative images of aorta (A, B, C), esophagus (D, E, F), bladder (G, H, I), and esophageal blood vessels (J, K, L) that were stained with periodic acid-Schiff reagents to detect glycogen. Discreet glycogen deposits (black arrows) are observed in smooth muscle of the vasculature, gastrointestinal tract, and genitourinary system of *Gaa*$^{-/-}$ mice at both 6 and 15 months of age, whereas WT mice lack accumulated glycogen. Scale bar=0.2 μm.

esophagus and bladder have even larger and darker PAS+ puncta; although there is not an increase in either the number or size of glycogen deposits in the aorta at this age. Interestingly, while we do not observe the expected gross glycogen accumulation in the aorta, it is observed in other blood vessels at both 6 and 15 months in *Gaa*$^{-/-}$ but not WT mice (Fig. 2J, K, L). There appear to be structural changes to the tunica media at 15 months, including widening of the layers and smoother appearance of the elastic lamina.

Vacuolar accumulation

Autophagy is the process by which nonfunctional organelles and bulk cytosol are selectively and non-selectively sequestered by an autophagosome, then delivered to the lysosome for degradation and nutrient recycling (28). Disruption of the autophagic pathway is a well-characterized cellular pathology in Pompe disease patient and murine model skeletal muscle (21, 25, 29, 30). As glycogen accumulates, lysosomes lose their ability to fuse with new autophagosomes, which then begin to accumulate. Cumulatively, vacuolar accumulation results in mechanical stress which weakens and damages the muscle fibers. Here, we sought to understand if vacuolar accumulation is also a pathological feature in smooth muscle. To do so, we quantified LAMP1—a lysosomal membrane protein—and LC3—an autophagosomal membrane protein—by western blot (Fig. 3, Supplemental Fig. 1). LC3 exists in two forms—LC3-I and LC3-II. LC3-I is found in the cytosol in low levels when autophagy is not active. Once autophagy is activated, LC3-I is lipidated to become LC3-II, then inserted into a growing autophagosomal membrane. In the aorta, esophagus, stomach, and bladder, significantly higher levels of LAMP1 are present in *Gaa*$^{-/-}$ mice, compared to WT. While increased levels of LAMP1 were measured in the trachea, it did not reach significance. The LC3-II/LC3-I ratio, an indicator of accumulated autophagosomes, is more variable among the tissues. A significantly higher ratio is observed in the esophagus and bladder of *Gaa*$^{-/-}$ mice, and a non-significant increased ratio trend is observed in the aorta and trachea.

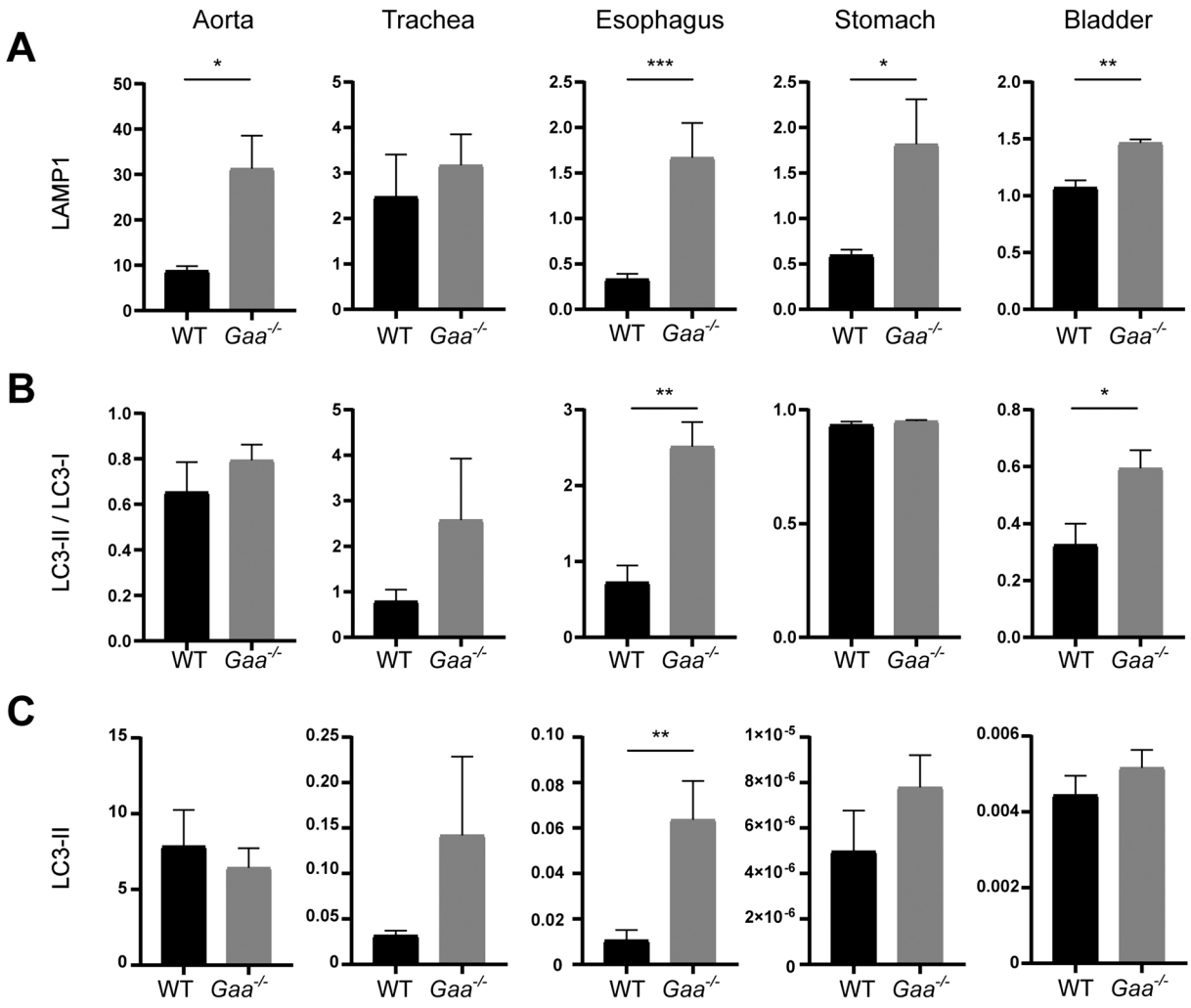

Fig. 3. LAMP1 and LC3 accumulation in 6 month old *Gaa*$^{-/-}$ mouse smooth muscle-containing tissues. (A) Quantification of band intensity on western blot probed with an antibody to LAMP1, a lysosomal membrane protein. As expected in Pompe disease there is an abundance of LAMP1 likely due to increased lysosomes in smooth muscle. (B) Ratio of quantification of western blot band intensities of LC3-II – autophagosome membrane protein, to LC3-I – the cytosolic precursor protein. (C) Quantification of western blot band intensities of LC3-II. Together, the ratio of LC3-II/LC3-I and the LC3-II alone indicates that there are variable levels of autophagosome accumulation in the smooth muscle of *Gaa*$^{-/-}$ mice. n=3–6 per group. Error bars represent mean ± SEM. **P*<0.05, ***P*<0.01, ****P*<0.001.

In the stomach, the ratio in the *Gaa*$^{-/-}$ mice is relatively similar to that in WT mice. The normalized values of LC3-II alone can also provide insight into autophagosome accumulation (Fig. 2C). In the esophagus, there is a statistically significant increase in LC3-II, and in the trachea, stomach, and bladder there is a trend of increased LC3-II in *Gaa*$^{-/-}$ mice compared to WT. In the aorta however, levels are nearly equivalent.

To better understand the status of autophagy in the smooth muscle cells of the most affected tissues—esophagus, stomach, and bladder—sections of each were stained for LAMP1 and LC3 (Fig. 4). In all three tissues, an abundance of discrete LAMP1+ puncta are present in *Gaa*$^{-/-}$ mice, whereas WT mice have none. In the esophagus and stomach, relatively large discrete LC3+ puncta are also present with smaller puncta present in the bladder of *Gaa*$^{-/-}$ mice. These puncta are absent in WT mice. We observe minimal overlap between lysosomes (LAMP1+ puncta) and autophagosomes (LC3+ puncta) indicating abnormal autophagosome maturation to autolysosomes in *Gaa*$^{-/-}$ mice.

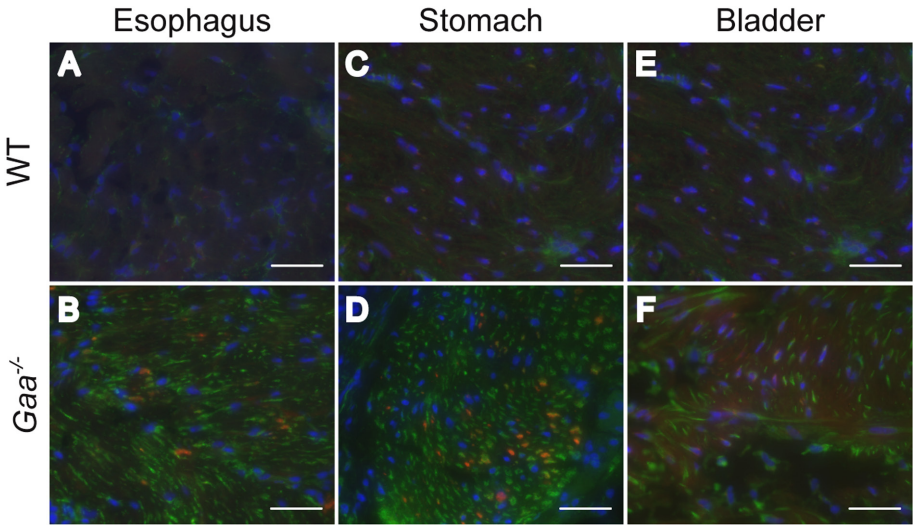

Fig. 4. Vacuolar accumulation in 6 month old *Gaa*$^{-/-}$ mouse smooth muscle-containing tissues. Representative images of smooth muscle in the esophagus, stomach, and bladder from *Gaa*$^{-/-}$ and WT mice, stained with LAMP1 (green) and LC3 (red) antibodies. In each tissue of the *Gaa*$^{-/-}$ mouse there is an abundance of LAMP1+ puncta with fewer LC3+ puncta, indicating a significant accumulation of lysosomes and a moderate accumulation of autophagosomes compared to the WT tissues devoid of any positive staining. Scale bar=40 μm.

Discussion and Conclusion

To our knowledge, this is the first study to report autophagosome accumulation in smooth muscle across multiple tissues from the *Gaa*$^{-/-}$ mouse. Based on our findings in the *Gaa*$^{-/-}$ mouse, smooth muscle of the airways, vasculature, GI tract, and GU system is affected. Not only is there glycogen accumulation, resulting in enlarged lysosomes, but autophagosomes are also amassed in smooth muscle-containing tissues. Smooth muscle has a significant role in many of the major organ systems including the respiratory system, vasculature, gastrointestinal tract, and genitourinary system. Postmortem evaluation of Pompe patients with both severe and moderate phenotypes has indicated glycogen accumulation in tissues of these organ systems, which, together with the molecular and histological pathologies seen in *Gaa*$^{-/-}$ mice, may provide a rationale for some of the phenotypic consequences reported in Pompe patients (31–36).

The vascular system is greatly impacted by Pompe disease. While the aorta had the lowest glycogen content compared to other smooth muscle tissues, there is still significant glycogen present in the vasculature of *Gaa*$^{-/-}$ mice. PAS+ puncta are observed throughout the tunica media similar to that observed in post-mortem evaluation of Pompe patients (34, 37). Interestingly, we find that smooth muscle cells lining small blood vessels in the esophagus (Fig. 2J, K, L), as well as in the bladder and tongue (data not shown) are even more densely packed with glycogen-filled lysosomes in *Gaa*$^{-/-}$ mice. Pompe patients experience aneurysm, dissection, and arteriopathy in the aorta, cerebral artery, renal artery, and the carotid artery, which lead to microhemorrhages, coma, and stroke (12, 17, 38–42). Among these, dilation of the basilar artery and aortic weakness are emerging as a common consequence, particularly among LOPD patients who have and have not received ERT (12–15, 17, 39, 40, 43–45). Interestingly, the limited PAS+ present at both 6 and 15 months in the aorta of *Gaa*$^{-/-}$ mice does not corroborate our hypothesis that glycogen accumulation is responsible for aortic wall weakness. We do note, however structural changes to the tunica media at 15 months which may indicate connective tissue pathology in the aorta that may contribute to the weakness observed in patients. Skin fibroblasts are widely used in

Pompe disease diagnosis and when they are cultured have significant levels of lysosomal glycogen. However, we do not find any reports of pathology in fibroblasts found in connective tissue; greater investigation into the role of fibroblasts in the aorta, and the impact of GAA-deficiency requires clarity.

Here, we find that *Gaa*$^{-/-}$ mice have significant levels of glycogen in the trachea, in congruence with previous reports evaluating airway smooth muscle (19, 26). Within the trachea there is a non-significant trend toward an increase of LAMP1 and LC3, which indicate some vacuolar enlargement and accumulation, as observed in skeletal muscle (21, 46, 47). This pathology mimics that observed in the bronchi of three infantile-onset Pompe patients, all of whom required ventilator support and experienced obstructive sleep apnea (31).

Representative tissues of the GI & GU systems—esophagus, stomach, and bladder have substantial lysosomal glycogen accumulation. GI and GU smooth muscle are the most impacted smooth muscle tissues of those analyzed in this study. In addition to glycogen, they also have significantly more LAMP1 and a higher LC3 ratio, which are reflected in immunofluorescence staining demonstrating accumulated lysosomes and autophagosomes. These pathologies may help explain the symptoms reported by Pompe patients. Many of the symptoms associated with glycogen storage in the GI and GU tracts such as gastroesophageal reflux, abdominal pain, feeding difficulties, and urinary incontinence are often noted as poor quality of life measures (48–51). However, more severe symptoms within these tracts have also been reported, including chronic diarrhea and vomiting requiring nutritional support and leading to failure to thrive, and increased incidence of bladder infections (51–54).

In conclusion, GAA deficiency results in significant glycogen accumulation in the airway, vascular, GI and GU smooth muscle. In addition, we noted significant lysosomal and autophagosomal accumulation in the GI and GU smooth muscle, determined by both western blot quantification and immunofluorescence localization. These cellular pathologies in the *Gaa*$^{-/-}$ mouse mimic those observed in Pompe patients and may be the cause of smooth muscle weakness.

Author Contributions

Conceptualization: ALM, MKE. Data Curation: ALM, JSD, AMB. Formal Analysis: ALM, JSD, AMB. Funding Acquisition: ALM, MKE. Methodology: ALM, MKE. Supervision: MKE. Visualization: ALM. Writing–original draft: ALM. Writing–review & editing: ALM, JSD, AMB, LAP, LMS, MKE.

Funding

Funding from K08HD077040 (MKE), Derfner Foundation Award (ALM), R01HD099486 (MKE), NCBiotech/Pfizer Postdoctoral Fellowship (ALM) supported the novel findings presented in this review. The authors confirm independence from the sponsors; the consent of the article has not been influenced by sponsors.

References

1. Hers HG. alpha-Glucosidase deficiency in generalized glycogenstorage disease (Pompe's disease). Biochem J. 1963; 86: 11–6. [Medline] [CrossRef]
2. Byrne BJ, Kishnani PS, Case LE, Merlini L, Müller-Felber W, Prasad S, van der Ploeg A. Pompe disease: design, methodology, and early findings from the Pompe Registry. Mol Genet Metab. 2011; 103(1): 1–11. [Medline] [CrossRef]
3. Kishnani PS, Hwu WL, Mandel H, Nicolino M, Yong F, Corzo D, Infantile-Onset Pompe Disease

Natural History Study. Group A retrospective, multinational, multicenter study on the natural history of infantile-onset Pompe disease. J Pediatr. 2006; 148(5): 671–6. [Medline] [CrossRef]

4. DeRuisseau LR, Fuller DD, Qiu K, DeRuisseau KC, Donnelly WH Jr, Mah C, Reier PJ, Byrne BJ. Neural deficits contribute to respiratory insufficiency in Pompe disease. Proc Natl Acad Sci USA. 2009; 106(23): 9419–24. [Medline] [CrossRef]
5. van den Hout HMP, Hop W, van Diggelen OP, Smeitink JAM, Smit GPA, Poll-The BTT, Bakker HD, Loonen MCB, de Klerk JBC, Reuser AJJ, van der Ploeg AT. The natural course of infantile Pompe's disease: 20 original cases compared with 133 cases from the literature. Pediatrics. 2003; 112(2): 332–40. [Medline] [CrossRef]
6. Kishnani PS, Steiner RD, Bali D, Berger K, Byrne BJ, Case LE, Crowley JF, Downs S, Howell RR, Kravitz RM, Mackey J, Marsden D, Martins AM, Millington DS, Nicolino M, O'Grady G, Patterson MC, Rapoport DM, Slonim A, Spencer CT, Tifft CJ, Watson MS. Pompe disease diagnosis and management guideline. Genet Med. 2006; 8(5): 267–88. [Medline] [CrossRef]
7. Yang CF, Niu DM, Jeng MJ, Lee YS, Taso PC, Soong WJ. Late-onset Pompe disease with left-sided bronchomalacia. Respir Care. 2015; 60(2): e26–9. [Medline] [CrossRef]
8. Corti M, Liberati C, Smith BK, Lawson LA, Tuna IS, Conlon TJ, Coleman KE, Islam S, Herzog RW, Fuller DD, Collins SW, Byrne BJ. Safety of intradiaphragmatic delivery of adeno-associated virus-mediated alpha-glucosidase (rAAV1-CMV-hGAA) gene therapy in children affected by Pompe disease. Hum Gene Ther Clin Dev. 2017; 28(4): 208–18. [Medline] [CrossRef]
9. Prater SN, Banugaria SG, DeArmey SM, Botha EG, Stege EM, Case LE, Jones HN, Phornphutkul C, Wang RY, Young SP, Kishnani PS. The emerging phenotype of long-term survivors with infantile Pompe disease. Genet Med. 2012; 14(9): 800–10. [Medline] [CrossRef]
10. McCall AL, Salemi J, Bhanap P, Strickland LM, Elmallah MK. The impact of Pompe disease on smooth muscle: a review. J Smooth Muscle Res. 2018; 54(0): 100–18. [Medline] [CrossRef]
11. Brenn BR, Theroux MT, Shah SA, Mackenzie WG, Heinle R, Scavina MT. Critical airway stenosis in an adolescent male with Pompe disease and thoracic lordosis: a case report. A A Case Rep. 2017; 9(7): 199–203. [Medline] [CrossRef]
12. Miyamoto Y, Etoh Y, Joh R, Noda K, Ohya I, Morimatsu M. Adult-onset acid maltase deficiency in siblings. Acta Pathol Jpn. 1985; 35(6): 1533–42. [Medline]
13. Sandhu D, Rizvi A, Kim J, Reshi R. Diffuse cerebral microhemorrhages in a patient with adult-onset Pompe's disease: a case report. J Vasc Interv Neurol. 2014; 7(5): 82–5. [Medline]
14. Anneser JMH, Pongratz DE, Podskarbi T, Shin YS, Schoser BGH. Mutations in the acid α-glucosidase gene (M. Pompe) in a patient with an unusual phenotype. Neurology. 2005; 64(2): 368–70. [Medline] [CrossRef]
15. Refai D, Lev R, Cross DT, Shimony JS, Leonard JR. Thrombotic complications of a basilar artery aneurysm in a young adult with Pompe disease. Surg Neurol. 2008; 70(5): 518–20. [Medline] [CrossRef]
16. Kretzschmar HA, Wagner H, Hübner G, Danek A, Witt TN, Mehraein P. Aneurysms and vacuolar degeneration of cerebral arteries in late-onset acid maltase deficiency. J Neurol Sci. 1990; 98(2-3): 169–83. [Medline] [CrossRef]
17. Makos MM, McComb RD, Hart MN, Bennett DR. Alpha-glucosidase deficiency and basilar artery aneurysm: report of a sibship. Ann Neurol. 1987; 22(5): 629–33. [Medline] [CrossRef]
18. Kobayashi H, Shimada Y, Ikegami M, Kawai T, Sakurai K, Urashima T, Ijima M, Fujiwara M, Kaneshiro E, Ohashi T, Eto Y, Ishigaki K, Osawa M, Kyosen SO, Ida H. Prognostic factors for the late onset Pompe disease with enzyme replacement therapy: from our experience of 4 cases including an autopsy case. Mol Genet Metab. 2010; 100(1): 14–9. [Medline] [CrossRef]
19. Keeler AM, Liu D, Zieger M, Xiong L, Salemi J, Bellvé K, Byrne BJ, Fuller DD, ZhuGe R, ElMallah MK. Airway smooth muscle dysfunction in Pompe (*Gaa*$^{-/-}$) mice. Am J Physiol Lung Cell Mol Physiol. 2017; 312(6): L873–81. [Medline]

20. Raben N, Nagaraju K, Lee E, Kessler P, Byrne B, Lee L, LaMarca M, King C, Ward J, Sauer B, Plotz P. Targeted disruption of the acid alpha-glucosidase gene in mice causes an illness with critical features of both infantile and adult human glycogen storage disease type II. J Biol Chem. 1998; 273(30): 19086–92. [Medline] [CrossRef]

21. McCall AL, Stankov SG, Cowen G, Cloutier D, Zhang Z, Yang L, Clement N, Falk DJ, Byrne BJ. Reduction of Autophagic Accumulation in Pompe Disease Mouse Model Following Gene Therapy. Curr Gene Ther. 2019; 19(3): 197–207. [Medline] [CrossRef]

22. Falk DJ, Mah CS, Soustek MS, Lee KZ, Elmallah MK, Cloutier DA, Fuller DD, Byrne BJ. Intrapleural administration of AAV9 improves neural and cardiorespiratory function in Pompe disease. Mol Ther. 2013; 21(9): 1661–7. [Medline] [CrossRef]

23. Fraites TJ Jr, Schleissing MR, Shanely RA, Walter GA, Cloutier DA, Zolotukhin I, Pauly DF, Raben N, Plotz PH, Powers SK, Kessler PD, Byrne BJ. Correction of the enzymatic and functional deficits in a model of Pompe disease using adeno-associated virus vectors. Mol Ther. 2002; 5(5 Pt 1): 571–8. [Medline] [CrossRef]

24. Pauly DF, Fraites TJ, Toma C, Bayes HS, Huie ML, Hirschhorn R, Plotz PH, Raben N, Kessler PD, Byrne BJ. Intercellular transfer of the virally derived precursor form of acid alpha-glucosidase corrects the enzyme deficiency in inherited cardioskeletal myopathy Pompe disease. Hum Gene Ther. 2001; 12(5): 527–38. [Medline] [CrossRef]

25. Lim JA, Li L, Raben N. Pompe disease: from pathophysiology to therapy and back again. Front Aging Neurosci. 2014; 6: 177. [Medline] [CrossRef]

26. Keeler AM, Zieger M, Todeasa SH, McCall AL, Gifford JC, Birsak S, Choudhury SR, Byrne BJ, Sena-Esteves M, ElMallah MK. Systemic delivery of AAVB1-GAA clears glycogen and prolongs survival in a mouse model of Pompe disease. Hum Gene Ther. 2019; 30(1): 57–68. [Medline]

27. Mah C, Cresawn KO, Fraites TJ Jr, Pacak CA, Lewis MA, Zolotukhin I, Byrne BJ. Sustained correction of glycogen storage disease type II using adeno-associated virus serotype 1 vectors. Gene Ther. 2005; 12(18): 1405–9. [Medline] [CrossRef]

28. Yorimitsu T, Klionsky DJ. Autophagy: molecular machinery for self-eating. Cell Death Differ. 2005; 12(Suppl 2): 1542–52. [Medline] [CrossRef]

29. Fukuda T, Ewan L, Bauer M, Mattaliano RJ, Zaal K, Ralston E, Plotz PH, Raben N. Dysfunction of endocytic and autophagic pathways in a lysosomal storage disease. Ann Neurol. 2006; 59(4): 700–8. [Medline] [CrossRef]

30. Nascimbeni AC, Fanin M, Masiero E, Angelini C, Sandri M. The role of autophagy in the pathogenesis of glycogen storage disease type II (GSDII). Cell Death Differ. 2012; 19(10): 1698–708. [Medline] [CrossRef]

31. Pena LDM, Proia AD, Kishnani PS. Postmortem findings and clinical correlates in individuals with infantile-onset Pompe disease. JIMD Rep. 2015; 23: 45–54. [Medline] [CrossRef]

32. Hobson-Webb LD, Proia AD, Thurberg BL, Banugaria S, Prater SN, Kishnani PS. Autopsy findings in late-onset Pompe disease: a case report and systematic review of the literature. Mol Genet Metab. 2012; 106(4): 462–9. [Medline] [CrossRef]

33. Sacconi S, Bocquet JD, Chanalet S, Tanant V, Salviati L, Desnuelle C. Abnormalities of cerebral arteries are frequent in patients with late-onset Pompe disease. J Neurol. 2010; 257(10): 1730–3. [Medline] [CrossRef]

34. Goeber V, Banz Y, Kaeberich A, Carrel T. Huge aneurysm of the ascending aorta in a patient with adult-type Pompe's disease: histological findings mimicking fibrillinopathy. Eur J Cardiothorac Surg. 2013; 43(1): 193–5. [Medline] [CrossRef]

35. Bernstein DL, Bialer MG, Mehta L, Desnick RJ. Pompe disease: dramatic improvement in gastrointestinal function following enzyme replacement therapy. A report of three later-onset patients. Mol Genet Metab. 2010; 101(2-3): 130–3. [Medline] [CrossRef]

36. Chancellor AM, Warlow CP, Webb JN, Lucas MG, Besley GT, Broadhead DM. Acid maltase deficiency presenting with a myopathy and exercise induced urinary incontinence in a 68 year old male. J Neurol

Neurosurg Psychiatry. 1991; 54(7): 659–60. [Medline] [CrossRef]

37. El-Gharbawy AH, Bhat G, Murillo JE, Thurberg BL, Kampmann C, Mengel KEE, Kishnani PS. Expanding the clinical spectrum of late-onset Pompe disease: dilated arteriopathy involving the thoracic aorta, a novel vascular phenotype uncovered. Mol Genet Metab. 2011; 103(4): 362–6. [Medline] [CrossRef]
38. Huded V, Bohra V, Prajapati J, DeSouza R, Ramankutty R. Stroke in young-dilative arteriopathy: a clue to late-onset Pompe's disease? J Stroke Cerebrovasc Dis. 2016; 25(4): e50–2. [Medline] [CrossRef]
39. Pichiecchio A, Sacco S, De Filippi P, Caverzasi E, Ravaglia S, Bastianello S, Danesino C. Late-onset Pompe disease: a genetic-radiological correlation on cerebral vascular anomalies. J Neurol. 2017; 264(10): 2110–8. [Medline] [CrossRef]
40. Pappa E, Papadopoulos C, Grimbert P, Laforêt P, Bassez G. Renal artery fibromuscular dysplasia in Pompe disease: a case report. Mol Genet Metab Rep. 2018; 16: 64–5. [Medline] [CrossRef]
41. Hensel O, Hanisch F, Stock K, Stoevesandt D, Deschauer M, Müller T. Morphology and function of cerebral arteries in adults with pompe disease. JIMD Rep. 2015; 20: 27–33. [Medline] [CrossRef]
42. Quenardelle V, Bataillard M, Bazin D, Lannes B, Wolff V, Echaniz-Laguna A. Pompe disease presenting as an isolated generalized dilative arteriopathy with repeated brain and kidney infarcts. J Neurol. 2015; 262(2): 473–5. [Medline] [CrossRef]
43. Laforêt P, Nicolino M, Eymard PB, Puech JP, Caillaud C, Poenaru L, Fardeau M. Juvenile and adult-onset acid maltase deficiency in France: genotype-phenotype correlation. Neurology. 2000; 55(8): 1122–8. [Medline] [CrossRef]
44. Braunsdorf WE. Fusiform aneurysm of basilar artery and ectatic internal carotid arteries associated with glycogenosis type 2 (Pompe's disease). Neurosurgery. 1987; 21(5): 748–9. [Medline] [CrossRef]
45. Matsuoka Y, Senda Y, Hirayama M, Matsui T, Takahashi A. Late-onset acid maltase deficiency associated with intracranial aneurysm. J Neurol. 1988; 235(6): 371–3. [Medline] [CrossRef]
46. Shea L, Raben N. Autophagy in skeletal muscle: implications for Pompe disease. Int J Clin Pharmacol Ther. 2009; 47(Suppl 1): S42–7. [Medline]
47. Falk DJ, Todd AG, Lee S, Soustek MS, ElMallah MK, Fuller DD, Notterpek L, Byrne BJ. Peripheral nerve and neuromuscular junction pathology in Pompe disease. Hum Mol Genet. 2015; 24(3): 625–36. [Medline] [CrossRef]
48. Jones HN, Muller CW, Lin M, Banugaria SG, Case LE, Li JS, O'Grady G, Heller JH, Kishnani PS. Oropharyngeal dysphagia in infants and children with infantile Pompe disease. Dysphagia. 2010; 25(4): 277–83. [Medline] [CrossRef]
49. Gesquière-Dando A, Attarian S, Maues De Paula A, Pouget J, Salort-Campana E. Fibromyalgia-like symptoms associated with irritable bowel syndrome: a challenging diagnosis of late-onset Pompe disease. Muscle Nerve. 2015; 52(2): 300–4. [Medline] [CrossRef]
50. Pardo J, García-Sobrino T, López-Ferreiro A. Gastrointestinal symptoms in late-onset Pompe disease: early response to enzyme replacement therapy. J Neurol Sci. 2015; 353(1-2): 181–2. [Medline]
51. McNamara ER, Austin S, Case L, Wiener JS, Peterson AC, Kishnani PS. Expanding our understanding of lower urinary tract symptoms and incontinence in adults with pompe disease. JIMD Rep. 2015; 20: 5–10. [Medline] [CrossRef]
52. Ajay D, McNamara ER, Austin S, Wiener JS, Kishnani P. Lower urinary tract symptoms and incontinence in children with Pompe disease. JIMD Rep. 2016; 28: 59–67. [Medline] [CrossRef]
53. Thurberg BL, Lynch Maloney C, Vaccaro C, Afonso K, Tsai ACH, Bossen E, Kishnani PS, O'Callaghan M. Characterization of pre- and post-treatment pathology after enzyme replacement therapy for Pompe disease. Lab Invest. 2006; 86(12): 1208–20. [Medline] [CrossRef]
54. Remiche G, Herbaut AG, Ronchi D, Lamperti C, Magri F, Moggio M, Bresolin N, Comi GP. Incontinence in late-onset Pompe disease: an underdiagnosed treatable condition. Eur Neurol. 2012; 68(2): 75–8. [Medline] [CrossRef]